communications earth & environment

Article

https://doi.org/10.1038/s43247-024-01815-8

Deglaciation in the subtropical Andes has led to a peak in sediment delivery

Iván Vergara [1,2] ✉, René Garreaud[1,3], Ian Delaney[4] & Álvaro Ayala[5]

Glaciers are thinning and retreating as climate warms, thus eroding less of the Earth's surface. However, other hydrological factors in glacierized catchments are likely producing a transient increase in sediment delivery, resulting in 'peak sediment'. Estimating the trajectory of the peak sediment is ecologically and socially important but scientifically challenging because of the delayed and non-linear response of glacier sediment export to climate forcing. This study used time series of suspended sediment concentration starting in the 1960s from 11 Andean rivers at subtropical latitudes to analyse past changes in sediment export and infer its future behaviour. The recent decade has experienced anomalously high sediment concentration in most glacierized catchments, but the 1970s experienced even higher values. Decadal variations in the relationship between sediment concentration and ice melt suggest that the magnitude of the current decade was lower due to reduced glacial sediment rather than other factors. Combining this result with the fact that glacial runoff is decreasing, it is inferred that, for most of the glacierized catchments, the peak sediment generated by the anthropogenic deglaciation started two centuries ago has already passed its maximum.

Mountain glaciers have a great erosive capacity, contributing to topographic relief of the Earth[1]. Once glaciers produce sediment and solutes, these are displaced by the ice itself or by wind and water to lowlands, where they play a fundamental role in landform evolution, ecosystems and human activities such as water management and hydropower generation[2,3]. For example, in the subtropical Andes, decadal-scale increments in sediment export have had negative consequences on reservoir capacity and drinking water supply[4–6] and a potentially positive impact on coastal ecology due to greater availability of nutrients[7].

Climate warming is expected to decrease the erosive capacity of glaciers as they thin and retreat due to the reduced gravitational driving stress and sliding speeds, thus reducing sediment production[8–11]. However, glaciers' sediment export may increase after deglaciation begins due to the upstream extension of the subglacial hydrological system that connects long-term stored sediment[4,10,12] (Fig. 1). Similar to the concept of a transient increase in glacier runoff, known as 'peak water'[13], this transient increase in sediment export was termed as 'peak sediment'[14,15]. Peak sediment depends mainly on climate variability, glacier thermal regime, bed topography, and the mass and distribution of stored sediment. For a typical valley glacier, it can last for more than a century and extend beyond the peak water[10,16]. In line with the theory of peak sediment[14], the global, present-day deglaciation, which started approximately in the 19th century due to anthropogenic warming[17], is driving an increase in sediment export from several glacierized regions, such as the Andes, European Alps, Artic, and Himalayas[18–20]. Similarly, climate warming is also expected to generate a transient rise in sediment production in the periglacial environment and a transition in the sediment transport regime of mountain rivers from thermal to pluvial[3,21].

Despite knowledge of glacier and hydrology's evolution in response to climate warming, evaluating the timing of peak sediment remains difficult because glaciers' thermal regime, stored subglacial sediment, and hydro-sedimentological connectivity are usually unknown. Notwithstanding these difficulties, peak sediment is projected to end between 2100 and 2200 globally[15]. In contrast, another study suggests that two alpine catchments are currently experiencing their maximum and will end between 2070 and 2100[22].

Here, six-decade-long sediment discharge series of eleven subtropical Andean rivers between 27 and 35 °S were used to shed light on future glacier sediment export (Fig. 2a and Table S1). In particular, the evolving relationship between water and sediment released by glaciers was evaluated from the 1960s onwards. This relationship yields insights into the temporal evolution of glacial sediment availability in response to changing glaciological, climatic and hydrology forcing. The rivers' catchments contain variable ice volume, but, without exception, gauges are between a few tens and hundred kilometres away from glaciers' terminus. Gauges measure suspended sediment concentration and mass in the stream. We focus on the suspended sediment concentration (SSC, mg l^{-1}) because the sediment mass

[1]Center for Climate and Resilience Research, Santiago, Chile. [2]IPATEC, CONICET-UNCo, Bariloche, Argentina. [3]Department of Geophysics, University of Chile, Santiago, Chile. [4]Institut des dynamiques de la surface terrestres (IDyST), Université de Lausanne, Lausanne, Switzerland. [5]Centro de Estudios Avanzados en Zonas Áridas (CEAZA), La Serena, Chile. ✉e-mail: ivergara@comahue-conicet.gob.ar

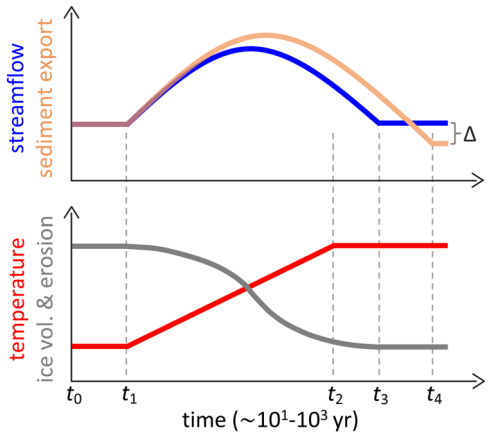

Fig. 1 | Schematic illustration of how peak sediment occurs. Assuming constant precipitation accumulation and intensity, a linear, secular temperature rise decreases glacial erosion by reducing the thickness and basal velocity[9,42,50]. Deglaciation, in turn, produces a transient increase in streamflow by releasing stored water (t_1-t_3) and in sediment flux, mainly due to the augmented accessibility of meltwater along the glacial bed that connects stored till (t_1-t_4; other studies refer to the peak sediment as the maximum value of the disturbance)[14]. Ice volume and streamflow may decrease after temperature stabilisation if the glacier is out of balance with climate (t_2-t_3)[51]. At t_3, we assume the glacier reaches a new equilibrium but could also disappear[13]. At t_4, sediment flux is lower than in period t_0-t_1 because the thinner glacier erodes less. Note that depending on glacier characteristics and the duration and magnitude of the temperature increase, the behaviour of the other plotted variables may change.

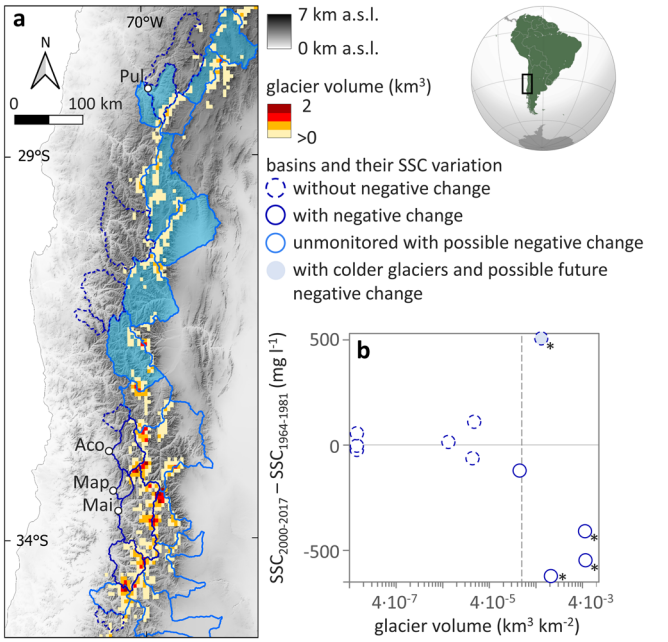

Fig. 2 | Study area and its glacio-sedimentary context. a Basins analysed and ice volume at a resolution of 0.05°[52]. The basins' outlines indicate the presence of SSC records and whether a significant change in mean annual SSC of the period 2000–2017 was identified in relation to the period 1964–1981. The location of the Aconcagua (Aco), Mapocho (Map), Maipo (Mai) and Pulido (Pul) basins is specified. **b** Relationship between ice volume and basin SSC changes between the periods 2000–2017 and 1964−1981. The vertical dashed line indicates the threshold mentioned in the Discussion, and asterisks indicate significant SSC changes at the 95% level. The SSC values were calculated for the warm and dry seasons from October to March. The same pattern persists for annual values, although fewer rivers have sufficient measurements (Fig. S1).

transported by glacial meltwater in the region is comparable in magnitude to that generated by snowmelt outside glaciers, but usually has a higher solid:liquid ratio as it circulates over the sediment-rich glacial bed[23]. In addition, snowmelt events produce more water and stream power than ice melt events[24], so they have more sediment from the bed and banks of the mainstem.

Subtropical andean glaciers

This high terrain has glaciers with both cold and polythermal regimes, including valley glaciers of up to 24 km^2 and surface velocities of up to ~300 m yr^{-1} in the 2010s[25–27]. In the glacierized Maipo River basin, located in the central-southern sector of the study area (Fig. 2a), there was a sharp increase in the mean and extreme turbidity during the warm and dry seasons of the last decade[4]. The positive interannual correlation of turbidity with ice melt, insignificant with rainfall, and negative with snowmelt outside or over glaciers allowed to link this increase to changes in the connectivity of the subglacial and proglacial areas, as these are the sources of sediment whose transport would be favoured by an increase in glacial streams[28]. This interpretation was also based on (a) the low land use change[4], (b) the absence of GLOFs in the catchment since 1954[29], and (c) the low frequency of slope instability associated with permafrost degradation and glacial retreat[30].

Results

Regime detection

By applying a sequential "regime shift" detection method[31] to the annual series of the three glacierized catchments with the most complete records, we identified three regimes or periods with specific SSC values (Methods). A high SSC regime is observed from the late 1960s until the mid-1970s (I), followed by a low SCC regime from the late 1970s to the 2000s (II), and then a new high SSC regime in the 2010s (III) (Fig. 3a–c). Interestingly, SSC values during regime III are about half of those of the first period in the 1970s. When including the remaining catchments in the analysis, it is observed that the higher magnitude of SSC during the first period occurs only in glacierized catchments (Fig. 2b).

The change between regimes II and III corresponds to the sharp increase in turbidity in the Maipo River. Although regime I was not previously analysed, judging from its below-average precipitation, like regime III[32] (Fig. 3d), and the pattern shown in the scatterplot of Fig. 2b, it is likely to have a cryospheric origin, similar to regime III. However, despite its possible common origin with the current high SSC regime, regime I has a higher magnitude which could be due to three potential temporal changes: a) exhaustion of sediment stored, b) diminished meltwater accessibility to sediment along the glaciers' bed because of lesser development of glacio-hydrological morphologies like moulins and supra- and sub- glacial channels, and c) decreased glacier water discharge and associated sediment transport capacity[16] because of diminished glacier area or climatic forcing (i.e., lower temperature and higher snowfall inhibiting subglacial runoff).

Identifying which of the three processes, or their combination, determines the current state of glacial sediment transport can provide clues about future sediment flux from these catchments. For example, if the lower SSC magnitude of the current regime compared to regime I was caused by glacial sediment exhaustion or a reduction in meltwater discharge due to the loss of glacier area, sediment export would be expected to decrease in the future. On the contrary, if the lower SSC magnitude of the current regime was because climatic forcing or meltwater accessibility were lower compared to regime I, sediment export could increase if these variables also do so.

Analysis of the regimes

To understand SSC changes, we first examine the magnitude and causes of variations in glacier runoff using annual estimates of ice melt and glacier area in the Maipo River basin. This is the only basin for which these outputs are available and it has similar topographic and climatic characteristics to the other basins in the south of the study area (Fig. 3c; Table S1). Both data come from glacio-hydrological simulations using the TOPKAPI-ETH model, which was run using geodetic glacier mass balance, remotely sensed snow cover area, local hydro-meteorological measurements, and an

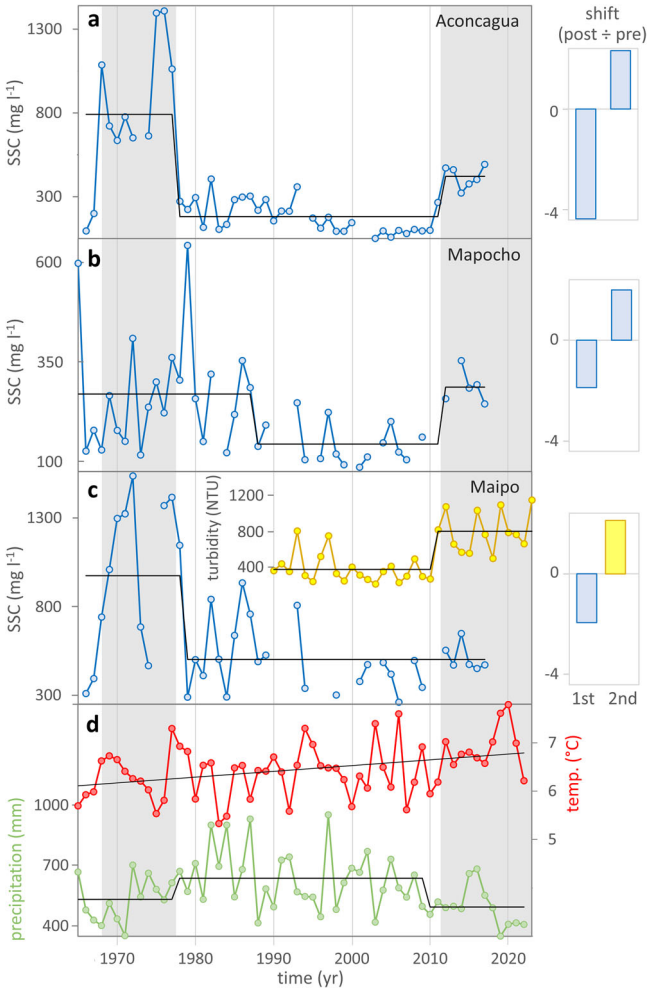

Fig. 3 | Interannual series of sediment export and climatic conditions. Average SSC for the rivers (**a**) Aconcagua, (**b**) Mapocho, and (**c**) Maipo, derived from monthly averages (Methods). The turbidity of the Maipo River is also plotted in (**c**). Regime shifts significant at the 95% level are represented by black lines, and their ratios are shown on the right. Similar patterns are observed when the median is considered (Fig. S2). **d** Average temperature and precipitation in box 27–35 °S, 69–72 °W obtained from the ERA5-Land reanalysis. Changes in temperature (precipitation) are represented by linear regression (temporal averages). Grey rectangles correspond to regimes I and III in the series of panel (**a**), which is the most reliable due to the largest number of samples.

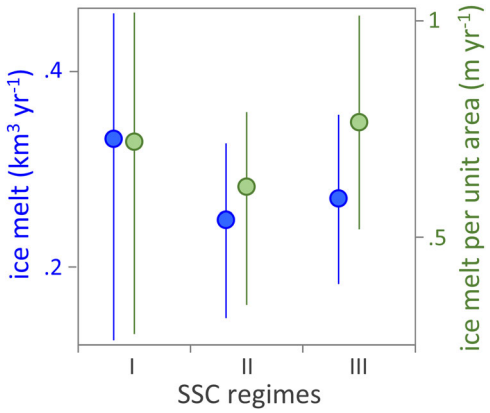

Fig. 4 | Ice melt conditions in the Maipo River basin during the SSC regimes I (1968−1977), II (1978–2010) and III (2011–2017). Points (lines) indicate averages (interquartile ranges). The values of regime III suggest a decrease in glacierized area and an increase in climatic forcing with respect to the first. The differences between the periods are not significant at a 95% level for any of the variables.

independent daily gridded snow water equivalent reconstruction[24]. This model was validated in the region against streamflow and snow cover area measurements, with satisfactory results, especially for annual integrations of the outputs such as those used here (24; Methods). For each SSC regime, annual averages of total ice melt and ice melt normalized per glacierized area were calculated. The total ice melt indicates the magnitude of glacial streamflow, whereas the specific ice melt expresses the climatic forcing strength and, indirectly, the connection between the atmosphere and subglacial system because it increases the development of glacio-hydrological morphologies[33]. When comparing the three regimes, the two high SSC periods experienced greater total and specific ice melt compared to regime II (Fig. 4). Yet, regime I had greater total melt and lower melt per unit area than regime III (Fig. 4). Although these differences are not significant at a 95% level, they are consistent with the larger glacierized area and the slightly colder and wetter climate during regime I in the 1970s[24,34] (Fig. 3d).

We assessed the role of sediment availability in the SSC changes by examining temporal variations in the interannual relationship between ice melt and the number of extreme turbidity events (ETE). The ETE were defined as days with SSC values above the 85th quantile during the warm and dry season (Methods). We used ice melt as a proxy for proglacial streamflow, and the number of ETE was used as a proxy for its SSC because glacial sediment evacuation is better detected in the right tail of the SSC probability distribution at gauges far from glaciers[4,35]. We only examined the frequency of the ETE, i.e., the number per year, to avoid bias caused by rainstorms, which produce SSC magnitudes much higher than purely thermal melting[4,36]. The ETE were calculated for the Aconcagua River basin, the glacierized catchment with the fewest measurement gaps, ensuring that results are independent of missing data (Fig. 3a; Table S1). This basin is adjacent to the Maipo River basin, where the ice melt data were calculated, and both basins have a high correlation in ice melt and sediment delivery (the number ETE calculated for the Maipo River basin were also tested; Methods). The relationship between ice melt and ETE frequency was evaluated through the coefficient of correlation (r) and the intercept and slope of their linear regression considering ice melt as a covariate. The r quantifies the relationship's strength, while the slope expresses the land erodibility, the shape and gradient of the channel, and the extent to which new sediment sources become available as streamflow rises[37–39]. The intercept indirectly indicates sediment availability because it is the minimum SSC value that streamflow can generate in the given context and is independent of its magnitude and increase[39].

The correlation r between ice melt and ETE during the two high SSC regimes (I and III) was positive, similar in magnitude and significantly different from the negative correlation during regime II (Fig. 5). The negative correlation signals that the ETE of that period were triggered by precipitation and snowmelt, and hence during years when a thick seasonal snowpack protected ice from summer temperatures and hindered the percolation of meltwater into glacial bed through moulins and crevasses[40,41]. The two high SSC regimes also have similar positive slopes in the relationship between ETE and ice melt, which are significantly steeper than those negative of the low SSC regime (Fig. 5). The higher slope indicates that ETE varied more strongly with ice melt over the high SSC regimes I and III compared to the low SSC regime II. Conversely, the intercept -a proxy of sediment availability when r is positive- was significantly higher during regime I and then it gradually decreased until the current regime when it slightly recovered (Fig. 5). The ongoing deglaciation and the higher specific ice melt of the current regime raise doubts that a lower accessibility of meltwater along glacial bed has caused this decrease. In turn, the likely lower magnitude of the glacial streamflow should not have modified the intercept of the relationship (Fig. 4). In this sense, the lower current sediment availability compared to regime I could be caused by exhausted glacial sediment. Combining this result with the fact that regional glacial water flux is decreasing[24], it is inferred that the peak sediment has largely passed its maximum and, therefore, glacier sediment flux will slowly decrease in the

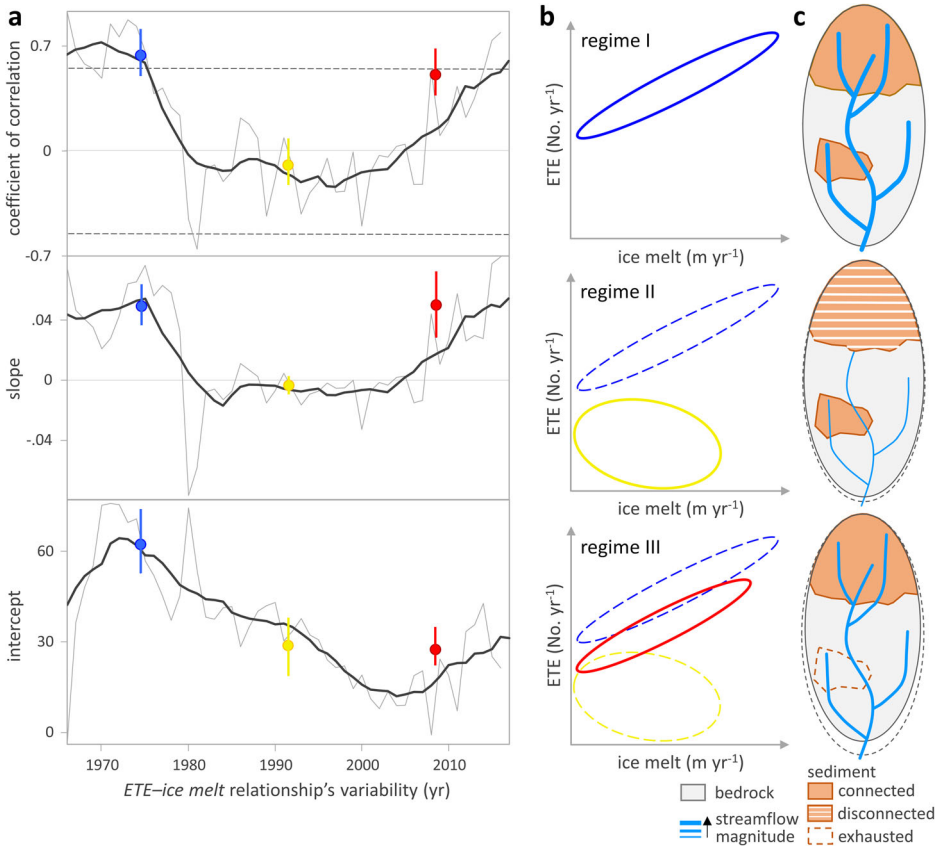

Fig. 5 | Glacio-sedimentary changes.
a Temporal variation in the relationship between glacial ice melt and ETE, for the Aconcagua River basin. Grey lines indicate 7-year sliding windows plotted in the middle year, and black lines represent their 9-year moving averages. Dashed, horizontal lines indicate significance at a 90% level, and points (vertical lines) indicate averages (interquartile ranges) for the three regimes. For the coefficient of correlation and slope, the II regime's average is significantly different from the other two at the 95% level. For the intercept, the I regime's average is significantly different from the other two at the 95% level. The same pattern is seen when other quantiles and variables are tested, including the ETE calculated for the Maipo River basin (Methods). **b** Conceptual scatterplots between ice melt and ETE during the regimes, where ellipses indicate scatter of points. **c** Conceptual models of how the bed of the glacier must have looked during the regimes.

future. Although, as mentioned above, sediment mass flux was not analysed in detail, its highest values during the 1970s and 1980s support this outcome (Fig. S3).

Discussion

A basin-scale relationship was detected between the long-term decrease of SSC and glacier volume (Fig. 2b). However, the northern Pulido River basin experienced an increase despite being noticeably glacierized (Fig. 2b). In comparison to the others that had decreased, this basin contains glaciers at a higher elevation and consequently colder and possibly with less meltwater in their bed (Table S1). Local studies corroborate that high-elevation northern glaciers have mostly cold thermal regimes[26,27]. In this sense, the glaciers of this basin may have been insensitive to the favourable conditions for increased sediment discharge of the 1970s. Therefore, in this basin, as in the others of its type, the peak sediment may not have passed its maximum yet (Fig. 2a). It must also be noted that, for basins with a preponderance of cold-based glaciers, peak sediment could be lower due to the possible less stored sediment associated with reduced sliding velocities as a result of decreased meltwater volumes[42].

The consistent findings across the catchments may suggest a regional pattern in sediment export. Considering unmonitored basins with a glacier volume greater than 2×10^{-4} km^3 km^{-2} (Fig. 2b) and an average glacial elevation less than that of the Pulido River basin, i.e., 5 km ASL, eight more basins of the size of those analysed may have had decreases in glacial sediment flux (Fig. 2a). If basins with higher glacial elevations are added to the analysis, it turns out that possibly most of the subtropical Andean rivers are experiencing or will experience during this century the maximum of the peak sediment (Fig. 2a).

The ice melt-ETE relationship shows a pronounced multidecadal variability, which would be due to the effects of regional climate and the memory of the glacio-hydrological system on the hydraulic connectivity of glacial sediment (Fig. 5). On the one hand, the natural decadal variability of the Pacific Ocean's climate, known as the Pacific Decadal Oscillation, results in periods of below (above) average precipitation[34,43] (Fig. S4) and, therefore, glaciers with less (more) snow accumulation and a subglacial realm more (less) connected to the atmosphere[40]. Nevertheless, years of high and low precipitation also occur during decades in which the opposite climatic situation predominates, suggesting that the variability of the ice melt-ETE relationship could also be caused by the multiannual memory of the glacio-hydrological system. For example, creating a moulin in the glacier's upper reaches would entail several years of negative mass balance in which each ablation season would begin from a point more advanced than the previous one[44–46]. In this context, a positive mass balance year might not close its roof with snow bridges that limit the access of meltwater to the glacier bed[47]. In the same way, during a period of positive and neutral mass balance years, a negative one could be insufficient for a new moulin to reach the glacier bed.

We propose that the observed changes in sediment export were mainly generated in the subglacial and proglacial environments. However, secondary sediment sources may include: a) the degrading permafrost[48], b) the occasional paraglacial landslides in the valley walls favoured by glacial unloading[30], and c) the GLOF of the early 1980s in the Cachapoal River basin (Table S1; 29), the only one in the study area since the 1960s.

Concluding remarks

Series of fluvial sediment concentration, unique in the world for their length and glacial information, were analysed to advance knowledge of a recently discovered cryospheric process called 'peak sediment'. This process is caused by global warming of recent centuries and has an important impact on hydropower generation, drinking water supply and river and coastal ecosystems. The results suggest that the peak sediment has passed its maximum for polythermal glaciers in the subtropical Andes but has not yet done so for colder glaciers at higher elevations. It was also observed that in addition to long-term trends, the sediment concentration of rivers has a substantial multidecadal variability controlled by regional climate and the

evolution of glacio-hydrologic morphologies. Therefore, the shape and timing of the peak sediment strongly depend on topography, climate and hydro-sedimentological connectivity, a fact that should be considered when inferring the state of other regions on the Earth.

Methods

River sediment data

Daily measurements of suspended sediment concentration (SSC; mg l^{-1}) derived from water samples at the Chilean gauging stations were obtained from the database of the Chilean Water Directorate (DGA; http://www.dga.cl/). SSC was sampled at the river surface and at approximately the same point using a bottle. The routine sampling procedure was the same for all the operators of the gauging stations[49]. The samples were filtered, ignited to remove organic matter, and weighed at the DGA laboratory[49]. To calculate the suspended sediment yield (SSY) of Fig. S3, the SSC measurements were multiplied by the concurrent streamflow measurements made by the DGA.

Once the data were downloaded, the gauges with 50% or more daily data in the period 1964–2017 were selected. The period was defined based on the hydrological annual cycle, which goes from April to March in the region. The *Río Illapel en las Burras* gauge was discarded despite having sufficient data due to its abnormal values possibly related to an error in field measurement, laboratory processing or measurement transcription (Sup. Material of Vergara et al.[23]).

For gaps of one day, data was filled with the average between the previous and following days. Following, monthly averages were calculated for those months with more than ten days of measurements. If the number of measurements was less, the average between the values of the same month of the previous and subsequent years was used, and failing that, the average between the last and following months of the same year. For year-round averages, years with less than ten months with more than ten daily measurements and at least one missing month that could not be filled by months of nearby hydrological years or months of the same year were discarded. For averages of the warm season, i.e., from October to March, those seasons with less than four months with more than ten measurements and at least one missing month that could not be filled with the other two methods were discarded. Emphasis was placed on this season because it is when the subglacial system is activated. In addition, sediment mass flux during the remaining months is much lower (Fig. 1c of Vergara et al.[4]).

To compare the averages of the periods 1964–1981 and 2000–2017 (Fig. 2b & S1), only gauges with at least six years with data in each period were used. This resulted in 9 gauges being used for the whole year and 11 for the warm season. All gauges are located between 27 and 35 °S (Table S1).

Ice melt data

To infer streamflow at the glacier snout, daily ice melt modelled for all glaciers in the Maipo River basin for the period 1955–2020 was used[24] (Table S1). This estimate was produced by the TOPKAPI-ETH model, a spatially distributed, physically oriented glacio-hydrological model suitable for calculating glacier mass balance and snow cover evolution in mountainous catchments. The model includes parameterizations of the most important hydrological processes at high altitudes, such as snow accumulation, albedo decay, snow gravitational redistribution, ice and snow melt, and ice melt under debris. Ayala et al.[24] applied numerous instances of the model to the study catchment, with spatial resolutions ranging from 100 m for glaciers (focusing on ice melt contribution and glacier mass balance) to 1 km for the whole catchment (focusing on seasonal snow cover). At each glacierized grid cell, the snow remaining at the end of each hydrological year is converted to ice. The main outputs of the model are the annual time series of glacier volume and area and the daily time series of rainfall, snowmelt and ice melt, which are further split into the fraction coming from glaciers and the one that comes from outside. For more information about the model applied, consult Ayala et al.[24].

Calculation of the regime shifts

For each series of Fig. 3, S2, S3 and S4a, temporal changes were assessed using the Sequential Regime Shift Detection method[31]. This technique is based on the calculation of a regime shift index combined with a sequential application of Student's *t*-tests to determine the significance and timing of regime shifts. Three parameters must be set to detect the regimes: the target significance level, the cut-off length and the outlier weighting factor (h). The significance level of the difference between mean values of neighbouring regimes is based on Student's two-tailed *t*-tests with unequal variance[31]. Regimes longer than the cut-off length will all be identified. Shorter regimes can also pass the test if the differences are large enough, but their detection depends on the selected Cut-off length and Significance level. The use of h allows for the detection of regimes unaffected by the influence of a single outlier with a disproportionate effect. Values outside $\pm h$ standard deviations will be weighted inversely proportional to their distance from the average of their corresponding regime.

We used a target significance level of 0.1, a cut-off length of 15 years considering the series lengths, and an h of 4, considering the series' high natural variability. Trials with different combinations of parameter values gave very similar results.

ETE calculation and their relationship to ice melt

The number of ETE were calculated for the warm season and the Aconcagua River basin (Fig. S4a), as the other highly glacierized basins have relatively few measurements (Table S1). Furthermore, its SSC data had the highest correlation with the reference turbidity series of the region, which has hourly resolution, has no gaps, and measures a fine grain size that is little influenced by stream power and more sensitive to hillslope and cryospheric processes (Fig. S6; Section 2.1 of Vergara et al.[4]). All this suggests that Aconcagua's temporal series best reflects how glacial sediment flux fluctuated and gives confidence about the results. Note that turbidity series could not be used to study long-term changes because it began operating in 1990 (Fig. 3a). A trial was performed calculating the ETE for the Maipo River basin, which gave similar results, especially for the intercept (Fig. S7).

To construct the ETE series, only warm seasons with at least 70% of daily data were used. In order to verify that rain played a minor role, a series of melt-driven ETE was generated, excluding days with precipitation, which gave similar results (Fig. S8 & Table S2). These account for 91% of the total. Although the scatterplot between ice melt and ETE suggests that the assumptions for a linear regression are not significantly violated (Fig. S9), the relationship was also analysed using a power law, which gave analogous results (Fig. S10).

Although the ETE and ice melt series correspond to different basins, it is important to note that the basins are adjacent and have similar hypsometries and glacier properties (Table S1). In fact, annual ice melt values of the Maipo basin glaciers and of the largest, most erosive glacier in the Aconcagua basin -the Juncal Norte- are highly correlated ($R^2 = 0.86$; Fig. S5; Sup. Note 1). Furthermore, as noted above, the SSC and turbidity of the basins also have a high interannual correlation amongst them (Fig. S6a, b).

Data availability

All databases used are publicly accessible. The daily SSC and streamflow records were obtained from the DGA website (http://www.dga.cl/servicioshidrometeorologicos/Paginas/default.aspx). ERA5-Land data were downloaded from Copernicus website (https://cds.climate.copernicus.eu/datasets/reanalysis-era5-land-monthly-means?tab=overview). The glacier volume data were downloaded from https://www.research-collection.ethz.ch/handle/20.500.11850/315707. The ice melt data are available in Vergara et al.[4]. The Regime Shift Detection Software was downloaded from https://sites.google.com/view/regime-shift-test/home?authuser=0.

Received: 20 June 2024; Accepted: 18 October 2024;
Published online: 26 October 2024

References

1. Herman, F., De Doncker, F., Delaney, I., Prasicek, G. & Koppes, M. The impact of glaciers on mountain erosion. *Nat. Rev. Earth Environ.* **2**, 422–435 (2021).
2. Li, D. et al. High Mountain Asia hydropower systems threatened by climate-driven landscape instability. *Nature Geoscience*. https://doi.org/10.1038/s41561-022-00953-y (2022).
3. Zhang, T. et al. Shifted sediment-transport regimes by climate change and amplified hydrological variability in cryosphere-fed rivers. *Sci. Adv*. https://doi.org/10.1126/sciadv.adi5019 (2023).
4. Vergara I., Garreaud R. & Ayala Á. Sharp increase of extreme turbidity events due to deglaciation in the subtropical Andes. *Journal of Geophysical Research: Earth Surface*. https://doi.org/10.1029/2021JF006584 (2022).
5. Rivera, J. A., Marianetti, G. & Scaglione, M. Assessment of precipitation events affecting the distribution of drinkable water in the Gran Mendoza area, Argentina. *Cuad. Geogr.áficos* **61**, 204–222 (2022).
6. Los Andes Newspaper 2022. https://www.losandes.com.ar/sociedad/dique-potrerillos-por-que-se-limpia-el-descargador-de-fondo-y-que-ocurriria-si-no-se-hiciera/.
7. Masotti, I. et al. The influence of river discharge on nutrient export and phytoplankton biomass off the Central Chile Coast (33°–37°S): Seasonal cycle and interannual variability. *Front. Mar. Sci.* **5**, 1–12 (2018).
8. Adhikari, S. & Marshall, S. J. Influence of high-order mechanics on simulation of glacier response to climate change: Insights from Haig Glacier, Canadian Rocky Mountains. *Cryosphere* **7**, 1527–1541 (2013).
9. Dehecq, A. et al. Twenty-first century glacier slowdown driven by mass loss in High Mountain Asia. *Nat. Geosci.* **12**, 22–27 (2019).
10. Delaney, I. & Adhikari, S. Increased Subglacial Sediment Discharge in a Warming Climate: Consideration of Ice Dynamics, Glacial Erosion, and Fluvial Sediment Transport. *Geophys. Res. Lett.* **47**, 1–11 (2020).
11. Jó, V., van Wyk de Vries, M., Ignéczi, Á., Mari, L., & Nagy, B. Glacier slowdown and rapid ice loss in the Tinguiririca and Cachapoal Basin, Central Andes of Chile. *Global and Planetary Change*, 231. https://doi.org/10.1016/j.gloplacha.2023.104287 (2023).
12. Schiefer, E., Hassan, M. A., Menounos, B., Pelpola, C. P. & Slaymaker, O. Interdecadal patterns of total sediment yield from a montane catchment, southern Coast Mountains, British Columbia, Canada. *Geomorphology* **118**, 207–212 (2010).
13. Huss, M. & Hock, R. Global-scale hydrological response to future glacier mass loss. *Nat. Clim. Change* **8**, 135–140 (2018).
14. Antoniazza, G. & Lane, S. N. Sediment yield over glacial cycles: A conceptual model. *Prog. Phys. Geogr.* **45**, 842–865 (2021).
15. Zhang, T. et al. Warming-driven erosion and sediment transport in cold regions. *Nat. Rev. Earth Environ.* https://doi.org/10.1038/s43017-022-00362-0 (2022).
16. Delaney, I., Anderson, L. & Herman, F. Modeling the spatially distributed nature of subglacial sediment transport and erosion. *Earth Surf. Dyn.* **11**, 663–680 (2023).
17. Masiokas, M. H. et al. Glacier fluctuations in extratropical South America during the past 1000 years. *Palaeogeogr., Palaeoclimatol., Palaeoecol.* **281**, 242–268 (2009).
18. Bendixen, M. et al. Delta progradation in Greenland driven by increasing glacial mass loss. *Nature* **550**, 101–104 (2017).
19. Li, D. et al. Exceptional increases in fluvial sediment fluxes in a warmer and wetter High Mountain Asia. *Science* **374**, 599–603 (2021).
20. Schmidt, L. K., Francke, T., Grosse, P. M., Mayer, C. & Bronstert, A. Reconstructing five decades of sediment export from two glacierized high-alpine catchments in Tyrol, Austria, using nonparametric regression. *Hydrol. Earth Syst. Sci.* **27**, 1841–1863 (2023).
21. East, A. E. & Sankey, J. B. Geomorphic and sedimentary effects of modern climate change: Current and anticipated future conditions in the western United States. *Rev. Geophysci.* 58. https://doi.org/10.1029/2019RG000692 (2020).
22. Schmidt, L. K., Francke, T., Grosse, P. M. & Bronstert, A. Projecting sediment export from two highly glacierized alpine catchments under climate change: exploring non-parametric regression as an analysis tool. *Hydrol. Earth Syst. Sci.* **28**, 139–161 (2024).
23. Vergara, I., Garreaud, R., Araneo, D. & Leyton, F. Environmental control of the present-day sediment export along the extratropical Andes. *Geomorphology* **441**, 1–9 (2023).
24. Ayala, Á. et al. Glacier runoff variations since 1955 in the Maipo River basin, semiarid Andes of central Chile. *The Cryosphere*, 1–39. https://doi.org/10.5194/tc-2019-233 (2020).
25. Millan, R., Mouginot, J., Rabatel, A. & Morlighem, M. Ice velocity and thickness of the world's glaciers. *Nat. Geosci.* **15**, 124–129 (2022).
26. Gacitúa, G. et al. 50 MHz helicopter-borne radar data for determination of glacier thermal regime in the central Chilean Andes. *Ann. Glaciol.* **56**, 193–201 (2015).
27. Masiokas, M. H. et al. A Review of the Current State and Recent Changes of the Andean Cryosphere. *Front. Earth Sci.* 8. https://doi.org/10.3389/feart.2020.00099 (2020).
28. Lane, S. N., Bakker, M., Gabbud, C., Micheletti, N. & Saugy, J.-N. Sediment export, transient landscape response and catchment-scale connectivity following rapid climate warming and alpine glacier recession. *Geomorphology* **277**, 210–227 (2017).
29. Iribarren Anacona, P., Mackintosh, A. & Norton, K. P. Hazardous processes and events from glacier and permafrost areas: Lessons from the Chilean and Argentinean Andes. *Earth Surf. Process. Landf.* **40**, 2–21 (2015).
30. Sepúlveda, S. A., Tobar, C., Rosales, V., Ochoa-Cornejo, F. & Lara, M. Megalandslides and deglaciation: modelling of two case studies in the Central Andes. *Nat. Hazards* **118**, 1561–1572 (2023).
31. Rodionov, S. N. A sequential algorithm for testing climate regime shifts. *Geophys. Res. Lett.* **31**, L09204 (2004).
32. Masiokas, M. H., Villalba, R., Luckman, B. H. & Mauget, S. Intra- to Multidecadal Variations of Snowpack and Streamflow Records in the Andes of Chile and Argentina between 30° and 37°S. *J. Hydrometeorol.* **11**, 822–831 (2010).
33. Rawlins, L. D., Rippin, D. M., Sole, A. J., Livingstone, S. J. & Yang, K. Seasonal evolution of the supraglacial drainage network at Humboldt Glacier, northern Greenland, between 2016 and 2020. *Cryosphere* **17**, 4729–4750 (2023).
34. Garreaud, R. D. et al. The Central Chile mega drought (2010–2018): A climate dynamics perspective. *Int. J. Climatol.* **40**, 421–439 (2020).
35. Skålevåg, A., Korup, O. & Bronstert, A. Inferring sediment-discharge event types in an alpine catchment from sub-daily time series, *Hydrol. Earth Syst. Sci*. [preprint], https://doi.org/10.5194/hess-2023-300 (2024).
36. Vergara, I., Garreaud, R., Moreiras, S., Araneo, D. & Beigt, D. Exploring the association between landslides and fluvial suspended sediment in a semi-arid basin in central Chile. *Geomorphology* **402**, 108129 (2022).
37. Asselman, N. E. M. Fitting and interpretation of sediment rating curves. *J. Hydrol.* **234**, 228–248 (2000).
38. Yang, G. et al. Sediment rating parameters and their implications: Yangtze River, China. *Geomorphology* **85**, 166–175 (2007).
39. Swift, D. A. et al. The hydrology of glacier-bed overdeepenings: Sediment transport mechanics, drainage system morphology, and geomorphological implications. *Earth Surf. Process. Landf.* **46**, 2264–2278 (2021).

40. Fountain, A. Effect of snow and firn hydrology on the physical and chemical characteristics of glacial runoff. *Hydrological Process.* **10**, 509–521 (1996).
41. Lane, S. N. & Nienow, P. W. Decadal-scale climate forcing of Alpine glacial hydrological systems. *Water Resour. Res.* **55**, 2478–2492 (2019).
42. Cuffey, K. M. & Paterson, W. S. B. Basal Slip. In K. M. Cuffey, & W. S. B. Paterson (Eds.), *The physics of glaciers* (4th ed.). Burlington, MA: Butterworth-Heinemann (2010).
43. Jacques-Coper, M. & Garreaud, R. D. Characterization of the 1970s climate shift in South America. *Int. J. Climatol.* **35**, 2164–2179 (2015).
44. Fountain, A. G. & Walder, J. S. Water flow through temperate glaciers. *Rev. Geophys.* **36**, 299–328 (1998).
45. Catania, G. A. & Neumann, T. A. 2010. Persistent englacial drainage features in the Greenland Ice Sheet. *Geophys. Res. Lett.* 37. https://doi.org/10.1029/2009GL041108 (1998).
46. Irvine-Fynn, T. D. L., Hodson, A. J., Moorman, B. J., Vatne, G. & Hubbard, A. L. Polythermal glacier hydrology: A review. *Rev. Geophys.* **49**, 1–37 (2011).
47. Gulley, J. D., Benn, D. I., Müller, D. & Luckman, A. A cut-and-closure origin for englacial conduits in uncrevassed regions of polythermal glaciers. *J. Glaciol.* **55**, 66–80 (2009).
48. Tapia Baldis, C. & Trombotto Liaudat, D. Rockslides and rock avalanches in the Central Andes of Argentina and their possible association with permafrost degradation. *Permafr. Periglac. Process.* **30**, 330–347 (2019).
49. Tolorza, V. et al. Suspended sediments in Chilean rivers reveal low postseismic erosion after the Maule Earthquake (Mw 8.8) during a severe drought. *J. Geophys. Res. Earth* **124**, 1378–1397 (2019).
50. Herman, F. et al. Erosion by an Alpine glacier. *Science* **350**, 193–195 (2015).
51. Mernild, S. H., Lipscomb, W. H., Bahr, D. B., Radić, V. & Zemp, M. Global glacier changes: A revised assessment of committed mass losses and sampling uncertainties. *Cryosphere* **7**, 1565–1577 (2013).
52. Farinotti, D. et al. A consensus estimate for the ice thickness distribution of all glaciers on Earth. *Nat. Geosci.* **12**, 168–173 (2019).

Acknowledgements

I.V. and R.G. are partially supported by CR2 - FONDAP/ANID 1522A0001. I.D. is funded by SNF Project No. PZ00P2_202024.

Author contributions

I.V. and R.G. designed the study. I.V. conducted the analyses. A.A. calculated the ice melt of the Juncal Norte glacier. I.V., R.G., I.D. and A.A. interpreted the analyses and contributed to the paper writing.

Competing interests

The authors declare no competing interests.

Additional information

Supplementary information The online version contains supplementary material available at https://doi.org/10.1038/s43247-024-01815-8.

Correspondence and requests for materials should be addressed to Iván Vergara.

Peer review information *Communications Earth & Environment* thanks Ting Zhang, Caio Breda and the other, anonymous, reviewer for their contribution to the peer review of this work. Primary Handling Editor: Carolina Ortiz Guerrero. A peer review file is available.